JOURNAL OF THERMOPHYSICS AND HEAT TRANSFER
Vol. 17, No. 1, January–March 2003

Radiative Heat Transfer in Film-Cooled Liquid Rocket Engine Nozzles

T. Badinand* and T. H. Fransson†
Royal Institute of Technology, 100 44 Stockholm, Sweden

A radiation model has been implemented in a Navier–Stokes flow solver to investigate the importance of thermal radiation in film-cooled liquid hydrogen/liquid oxygen rocket engine thrust chambers. Two running conditions were computed: high-altitude and sea-level conditions. For high altitudes, the walls are heated by radiation approximately 3 K, and the flow is not influenced. At sea level, the flow separates from the nozzle walls and a Mach disk is formed inside the nozzle. This extra source of radiation is clearly observable and, combined with the cold atmospheric air pocket created behind the separation, contributes importantly to the wall temperatures. An increase of up to 140 K is observed in the zone after the separation. Moreover, the position of the shock is slightly affected by radiative transfer. It is shown that radiative heat transfer does play an important role in the case of a shocked film-cooled nozzle. In the unshocked case, its effects are noticeable, but may be neglected.

Introduction

THE study of radiative heat transfer for liquid rocket engines started with the development of large-scale liquid rocket engines. One of the first examples of the importance of thermal radiation is the base heating mishaps that were observed during the development of the Saturn V rockets in the late 1950s.[1] It was shown that radiative heat transfer was one of the two main heating mechanisms. The same base heating mechanism was studied for the space shuttle's first and second stages some 20 years later.[2] A second important field where thermal radiation was admitted as a main heat transfer mechanism is reentry vehicles. Indeed, at hypersonic velocities, shocks are created in front of the spacecraft with appearance of large pressures, temperatures, and ionization of the medium. Those conditions create an important heat flux to the spacecraft forefront.[3] For internal heat transfer to the walls in nozzles, it was thought until recently that thermal radiation did not play a significant role for liquid oxygen/liquid hydrogen (LOX/LH) engines, with the main heat transfer to the nozzle walls occurring via convection. However, Nelson[4] showed for scramjet combustors that radiative heating represents roughly 10% of the convective heating, and Liu and Tiwari[5] found that radiative effects on the wall heat transfer may be significant in chemically reacting nozzle flows.

Today's rocket engine development is aimed at somewhat different goals than in the early space age. Whereas in the 1950s one wanted a successful launch at any cost, mostly driven by the cold war taking place between the Soviet Union and the United States, in the 1990s, space launch is mainly commercial. This means that the efficiency and the price per kilogram in orbit are of great importance. To decrease the second, two main research efforts are underway. The first one is the use of a reusable launcher. The space shuttle is the only commercially available launcher, but it is not competitive in price. While developing a reusable launch vehicle, the length of life of the main rocket engines is of great interest. Even if radiative heat transfer has a minor role compared to convection, perhaps it should not be neglected when a precise description is required of the heat loads to the nozzle walls for an engine that has to be restarted and that is aimed to several missions.

The second way to lower cost is to launch a heavier payload for a single launch. This implies more powerful rocket engines, which often imply bigger sizes, especially of the nozzle to use the maximum of energy generated by the combustion gases. Depending on the thermodynamic cycle chosen for the engine, either regenerative or film cooling can be used. For regenerative cooling, a coolant (often the fuel) is driven in the nozzle walls to lower their temperature. In this case, most of the heat is transferred via conduction through the wall and then convected away by the coolant. For gas generator cycles and when high thrust is required, film cooling has some advantages. Indeed, when film cooling is used, the losses due to friction on the nozzle wall are decreased. Also the exhaust gases from the turbine used in the film are more effectively expanded. However, the film only prevents convective heating from the hot gases. Because the gases in the film are not radiatively active (absorbing), the radiative heat to the walls is not affected by the film. In that case, radiative heat transfer may play a more important role.

Finally, the main engine is often used as primary propulsion when boosters have burnt out. This means that the highest thrust should be obtained at high altitudes. However, according to the thrust equation, the highest thrust is obtained when the gases are expanded to ambient pressure, which means very low pressure for high altitudes. Usually, the nozzles are designed for a mean altitude. As a consequence, the gases are under-expanded at sea-level conditions. This implies the emergence of shocks in the nozzle. The boundary layer on the nozzle wall separates, creating a shock starting at the wall and ending in the nozzle or at the exit with a Mach disk. The latter creates very high temperatures and pressures, extreme conditions where thermal radiation should play a major role not only for the wall heating mechanism, but also for the flowfield prediction in as much as shocks are sensible to heat fluxes.

The objective of the present paper is to assess the importance of radiative heat transfer for those different conditions where thermal radiation may play an important role in film-cooled LH/LOX engines. A radiative heat transfer code has been implemented in a general Navier–Stokes flow solver. The main characteristics of the radiation code will be presented, as well as a short description of the Navier–Stokes flow solver used. Flow predictions in a film-cooled nozzle follow, both in the case of high-altitude conditions and for underexpanded conditions where the boundary layer separates and a Mach disk is created in the nozzle. To the authors' knowledge, this is the first published computational study of radiative heat transfer in film-cooled shocked rocket nozzles. The present paper focuses on radiative heat transfer and will not give a detailed description of the computational fluid dynamics (CFD) calculation.

Received 31 January 2002; revision received 24 April 2002; accepted for publication 25 April 2002.

*Ph.D. Student, Chair of Heat and Power Technology, Brinellvägen 60; thomas.badinand.97@supaero.org. Student Member AIAA.

†Professor, Chair of Heat and Power Technology, Brinellvägen 60; fransson@egi.kth.se. Senior Member AIAA.

Numerical Method

Solving the Radiative Transfer Equation

The radiation phenomena in gases is ruled by the radiative transfer equation (RTE) expressing the conservation of energy applied to a monochromatic pencil of radiation propagating in an emitting, absorbing, and scattering medium. The equation is presented when scattering is neglected:

$$\frac{\mathrm{d}I_\nu}{\mathrm{d}s} = \boldsymbol{s}\cdot\nabla I_\nu = -\kappa_a I_\nu(\boldsymbol{R},\boldsymbol{s}) + \kappa_a I_{b,\nu}(\boldsymbol{R}) \tag{1}$$

where I_ν is the radiative intensity at wave number ν, $I_{b,\nu}$ the blackbody intensity for the same wave number, κ_a the absorption coefficient, s the direction, and R the position. This equation presents a challenge to solve both analytically and numerically due to the number of variables, three position, two direction, and one wave number, and its integro-differential character. Indeed, because radiation is traveling at the speed of light, no local conservation can be stated. Different methods have been applied to solve the RTE such as the zonal method, the Monte Carlo method, the discrete transfer method, the discrete ordinates method, and the finite volume method.[6] The latter has been chosen for this work because it is similar in philosophy to the Navier–Stokes solver. Indeed, it is based on a double discretization: The space is discretized in a finite number of cells (as well as for the flow solver), and the directional space is discretized in a finite number of solid angles. A complete description of the implementation of the solver may be found in Ref. 7. The main characteristics of the implementation are as follows. The step scheme is used for the interpolation from the nodes to the faces of a control volume because it was found to give good accuracy at low computational cost compared to a higher-order extrapolation.[8] To iterate, the volume cells of the domain are ordered for each direction from the most upstream to the most downstream. The solid angle overlapping a face is not solved because it was found to have little influence on the results.[7] The convergence criterion is a maximum relative change of the value of the radiative intensity in each cell between two consequent iterations less than 10^{-6}.

The solution of the RTE gives the radiative intensity I everywhere in the domain. To couple the radiation calculation with the flow calculation, the divergence of the radiative heat flux q_R is inserted as a source sink term in the energy equation[6] and is calculated as follows:

$$\nabla\cdot q_R = \int_0^\infty \kappa_\lambda \left[4\sigma T^4 - \int_{4\pi} I_\lambda \,\mathrm{d}\Omega\right]\cdot \mathrm{d}\lambda \tag{2}$$

where Ω is the solid angle, T the temperature, and σ the Planck constant. This term is based on the solution of the radiative intensity, which is obtained on a radiation spatial mesh coarser than the one used for CFD calculations. It is then interpolated to the CFD mesh as described in Ref. 9.

Solving the Nongrayness of the Gas

Equation 1 was written for a certain wave number, and the preceding paragraph described how to solve it for a single wave number. A very difficult subject in thermal radiation in gases is the dependency of the radiative intensity on the wave number. Indeed, gases absorb and emit only in lines at certain wave numbers, whereas solids emit along all wave numbers following Planck's law. The number of lines for each specie may be more than a million. If one wants to perform a very accurate calculation, the RTE has to be solved for each line [line-by-line method (LBL)], but this computation is obviously prohibitive in time. Then a technique has to be used to reduce the number of needed resolutions of the RTE. The spectral line-based weighted-sum-of gray gases with the absorption-line blackbody distribution function (ALBDF) as developed by Denisson and Webb[10] has been implemented. The advantage of the method is that the RTE has to be solved only few times (often between 3 and 20 times) giving, however, very accurate results when compared to LBL methods. It is estimated to be the best compromise between accuracy and computational time at the present time.[11] The main drawback of the method is the need for the definition of a reference state for which the absorption coefficients and the ALBDF are calculated. A new method was developed to reduce this problem in an inhomogeneous media with temperature and pressure gradients.[12] This method applied for rocket engines showed that, for a reasonable choice of the reference state, the uncertainty due to this reference state dependency could be assumed to be around ±5% (Ref. 13).

In the present work, only water vapor is considered as participating specie. The OH radiator is neglected, as in Ref. 5, because it is a much less active radiator than H_2O with a much lower concentration. Here, 20 gray gases and 1 transparent gas are used. The absorption coefficient is made dependent on temperature and pressure as explained earlier. Both absorption coefficients and values of the ALBDF are input as tables with values generated for 10 different pressures and 18 different temperatures. The high-temperature molecular spectroscopic database (HITEMP)[14] was used to generate those tables. The reference state is calculated as a volume mean of temperature, composition, and pressure weighted by the fourth power of the temperature and the radiating gas mole fraction.

Navier–Stokes Flow Solver

The Navier–Stokes flow solver used in the present work is an in-house code, VOLSOL, developed by Volvo Aero Corporation.[15] This is a multiblock, cell-centered finite volume code, where the convective flux is solved with an upwind-biased scheme and the diffusion terms with a compact second-order scheme. A three-stage Runge–Kutta algorithm is used to advance the solution in time. The code enables calculations of multispecie reacting flows. Finite reaction schemes are used for the combustion model. Turbulence is modeled with the k–omega turbulence model combined with the shear stress transport model.[16] Total variation diminishing (TVD) limiters are used to stabilize the calculation. The flow calculations were considered as converged when two solutions spaced by 5000 iterations had only negligible differences in mass fractions, temperature, pressure, density, and Mach number.

Estimation of Wall Temperature

During the simulations, radiation appears as a heat source in the flow, as already explained. In addition, radiation will influence wall temperatures. The strategy used to estimate the temperature increase due to radiation is, first, to consider adiabatic walls for convection, which means that the wall temperature during the flow calculation will be equal to the fluid temperature in the cell closest to the wall. Then from this solution, a heat flux balance is performed to estimate the new wall temperature. Because of the assumption of balanced flux, the new wall temperature will not influence the flow.

When Fig. 1 is considered, the heat balance equation can be stated as in Eq. (3). The heat coming from the gas side Q is equal to the conduction from the gases plus the absorbed radiative heat transfer to the wall: the impinging radiative heat flux q_R minus the emitted flux times the emissivity of the hot wall. This heat is then conducted through the wall and, finally, is equal to the heat lost on the cold side by convection and radiation:

$$\begin{aligned} Q &= k(T_h - T_{w,h}) + \varepsilon_h\left(q_R - \sigma T_{w,h}^4\right) = (\lambda_w/t_w)(T_{w,h} - T_{w,c}) \\ &= h_{cf}(T_{w,c} - T_c) + \varepsilon_c\sigma\left(T_{w,c}^4 - T_c^4\right) \end{aligned} \tag{3}$$

with

$$q_R = \int_{\Omega\, for\,(n\cdot s)<0} \int_{A_w} I(\boldsymbol{R},\boldsymbol{s})\cdot(\boldsymbol{n}\cdot\boldsymbol{s})\cdot \mathrm{d}A\,\mathrm{d}\Omega \tag{4}$$

where k is the gas thermal conductivity, h_{cf} the heat transfer coefficient of the coolant, A_w the surface area, and n the normal to the surface.

For all calculations where this heat balance is performed, the outside temperature T_c is taken to be 297 K, and the heat transfer coefficient on the cold side 50 W/m^2. The conductivity of the hot gas, k, has been evaluated using the following relation:

$$k = \lambda_{\mathrm{gas}}/\Delta y = C_{p,h}\cdot\mu_h/Pr\cdot\Delta y \tag{5}$$

where $C_{p,h}$ is the specific heat at constant pressure, μ_h the viscosity, and Pr the Prandtl number. Δy is taken equal to the distance between the center of the first cell and the wall.

Results and Analysis

Nozzle at Design Conditions

The general description of the nozzle studied is presented in Fig. 2. A two-dimensional axisymmetric mesh containing 35 blocks and 70,289 cells was generated. The mesh used for the radiation model consisted of 13,980 cells. The combustion chamber and the first part of the nozzle are regeneratively cooled, whereas the second part is film cooled. However, for the CFD calculation, all walls including the regeneratively cooled ones are considered as "convective adiabatic" walls. This means that the wall temperature is taken equal to the temperature in the cell nearest the wall. For the radiation calculation, the walls' regeneratively cooled temperatures are calculated with an external program developed for cooling calculations. The temperature given by the flow solver is used only for the film-cooled section. The atmosphere is taken as 100% nitrogen (N_2) to avoid afterburning. The atmosphere pressure is set to 40,000 Pa to simulate design conditions (high altitude). Notice an inflexion point in the nozzle bell shape. This was done to obtain a stable calculation in the case of overexpansion of the gases and to locate the appearing Mach disk inside the nozzle. For radiation, the emissivity of all walls is taken to be 0.4.

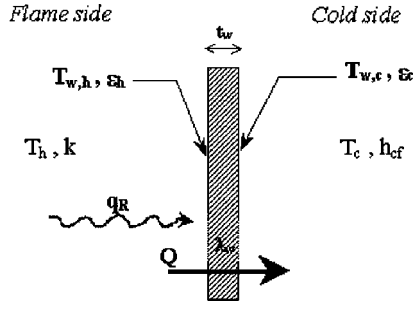

Fig. 1 Heat balance at the nozzle walls.

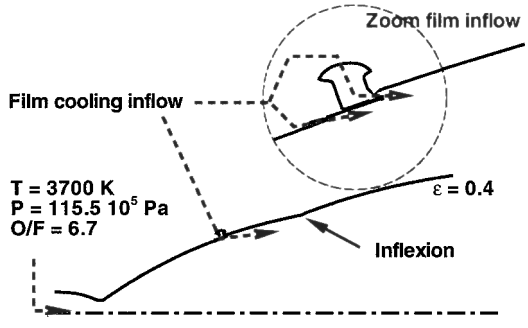

Fig. 2 Film-cooled nozzle.

Figure 3 shows the main variables of the flow: temperature, pressure, water vapor mole fraction, and Mach numbers obtained for a calculation without considering radiation. The dimensions on the axis are shown dimensionless. The flow is characterized by the expansion of the hot gases generated in the combustion chamber. Note that a separation appears at the end of the nozzle. This is because 40,000 Pa is still a too high ambient pressure for the flow. However, the flow inside the nozzle is quite unperturbed by it. For radiative heat transfer, the influencing variables are the high temperatures and pressures located before the throat and the quite uniform water vapor mole fraction in the high-temperature zones. The flow solution was coupled to the radiative solution, and the influence of radiation on the flow was found to be negligible.

Figure 4 shows the results obtained for the radiative heat transfer calculation for the film-cooled section. The wall temperatures are made dimensionless by dividing by the total temperature of the injected gases in the film. Three heat fluxes are plotted. The impinging radiative heat flux is the heat flux hitting the surface calculated according to Eq. (4), and the net radiative heat flux is the impinging heat flux lowered by the heat emitted by the surface. To obtain the heat absorbed by the material, this net heat flux should be multiplied by the emissivity (0.4 in this case). The last heat flux shown is the impinging heat flux originating from the walls (no emission from the gases). These results lead to the conclusion that most of the radiative heat flux (between 60 and 80%) comes from the gases. Looking at the shape of the emission (decreasing heat flux with increasing abscissa), it can be seen that most of the heat seems to originate from the throat and combustion chamber area where gases are at high pressures and temperatures. The heat absorbed by the surface is reduced when its temperature increases; however, radiation never cools the surface. The temperature that the surface should have to reach a negative radiative heat flux is around 1.8 times the injection temperature.

The surface is then heated by radiation. However, because of the relative low levels of the heat flux combined with the high conductivity of the hot gases, a temperature increase of 3–5 K is found until the separation zone at the extreme end of the nozzle. In this region, an increase of up to 40 K is due to the sinking conductivity

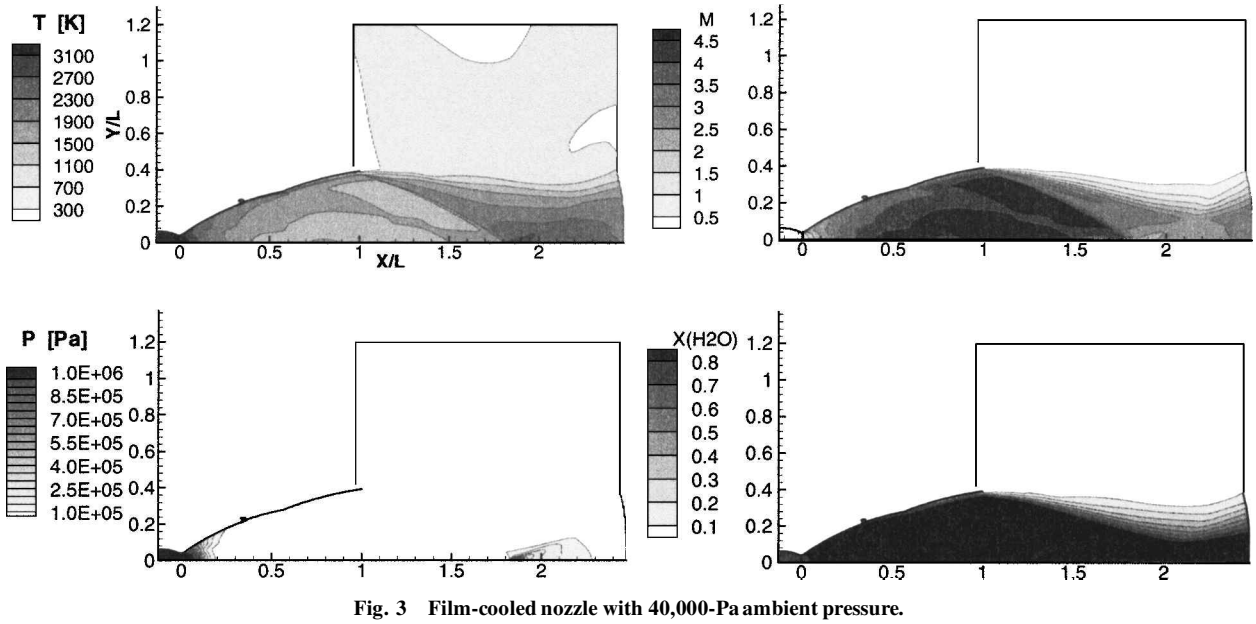

Fig. 3 Film-cooled nozzle with 40,000-Pa ambient pressure.

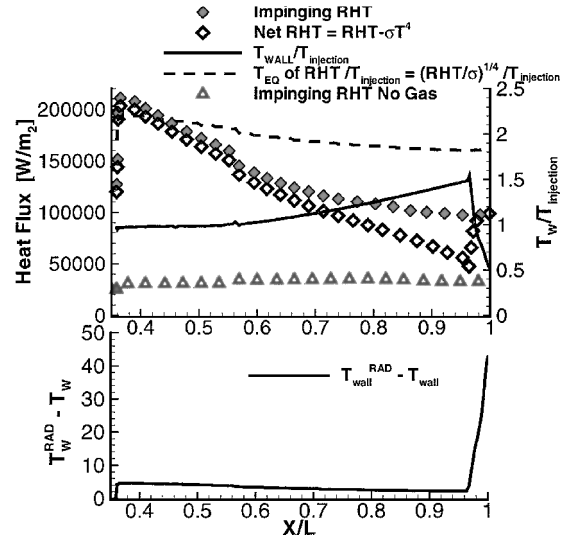

Fig. 4 Radiative heat flux and resulting wall temperatures for the high-altitude case.

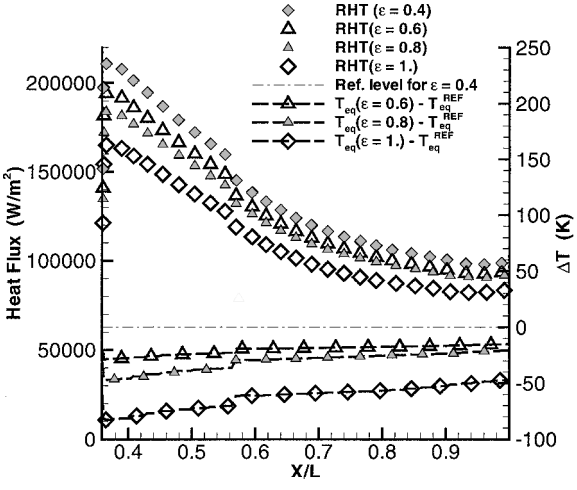

Fig. 5 Influence of the walls' emissivity on the radiative heat flux.

of the colder gases. This phenomenon is described more in detail in the next section. For normal running conditions, the wall temperature is then not significantly affected by radiation. For the radiation calculation, the surface's emissivity has been taken to 0.4. However, the walls in contact with the hot combustion products may be oxidized, and then their emissivity increases. The influence of this phenomenon on the film-cooled section is presented in Fig. 5.

The inlet section and the film-cooled surface's emissivity has been kept to 0.4 because they should not be oxidized. The other walls' emissivity (regeneratively cooled walls) has been increased to 0.6, 0.8, and 1. The influence on the equivalent temperature is shown. Because most of the radiative heat comes from the gases, increasing the wall's emissivity decreases the impinging heat flux. Indeed, a bigger part of the gas radiation is absorbed by the walls, which emit less radiation due to their low temperature (regeneratively cooled). Taking an emissivity of 0.6, 0.8, and 1 instead of 0.4 decreases the heat flux by approximately 5, 8, and 20%, respectively. The equivalent temperature is then lowered by around 10, 25 and 65 K. The conclusion is that the more the walls oxidize during the flight, the less heat is radiated to the film-cooled section.

In conclusion, at design running conditions, the radiative heat flux seems to have an observable but negligible effect on the film-cooled section of the nozzle.

Shocked Film-Cooled Nozzle

As explained in the Introduction, nozzles to LOX/LH engines are often designed for high altitudes because boosters give the main thrust in the first phase of flight. This is the case, for example, for the U.S. space shuttle, the European Ariane V, and the Chinese Long March rockets. This means that, at sea level, the gases in the nozzle are overexpanded. When the nozzle attains a large size, the gases are highly overexpanded, and then their only means to catch up the atmospheric pressure is via shocks.

The earlier described film-cooled geometry has been computed for an ambient pressure reproducing sea-level conditions: 10^5 Pa. The resulting flow is shown in Fig. 6. In this case, shocks appear near the inflexion point, involving separation of the nozzle wall boundary layer and then also the cooling film. A Mach disk is created in the nozzle at $x/L \sim 0.9$. For a precise description of the shock phenomenon taking place in rocket nozzles, the reader is invited to consult Refs. 17 and 18. For the flow, the shocks involve the appearance of a pocket of cold, slowly moving air (N_2 in the present calculation) in the nozzle after the separation. The flow before the shock system is similar to the case at high altitudes.

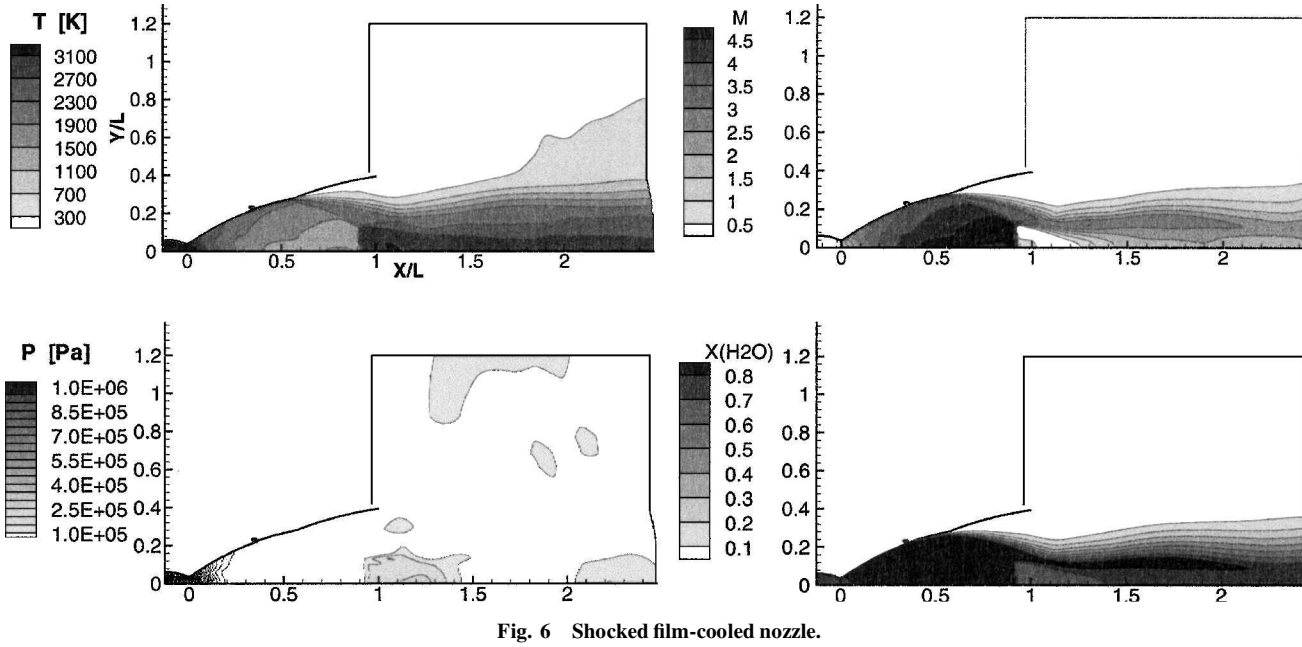

Fig. 6 Shocked film-cooled nozzle.

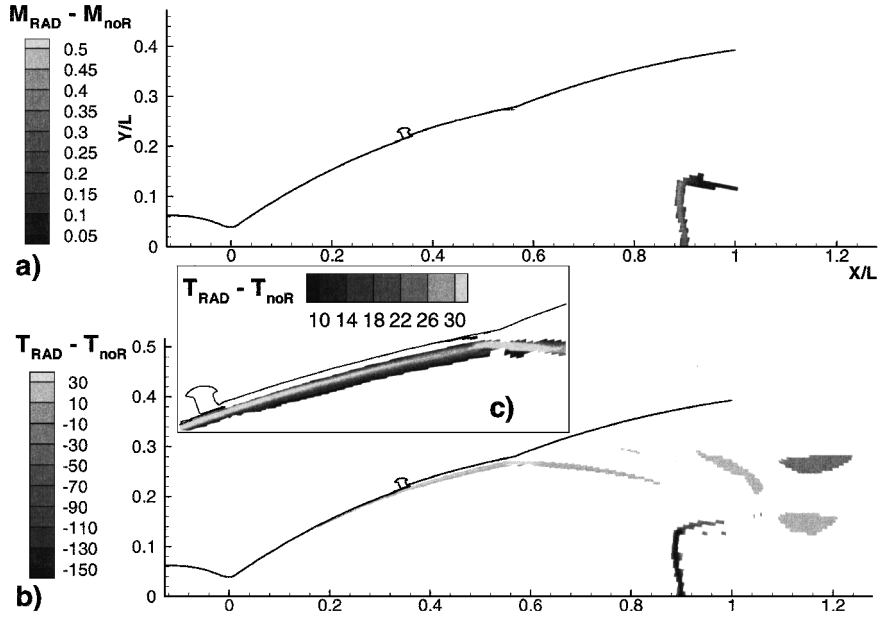

Fig. 7 Influence of radiation on the flowfield: a) the Mach difference if $|\Delta M| > 0.05$, b) temperature difference if $|\Delta T| > 10$ K, and c) zoom on film inlet for $|\Delta T| > 5$ K.

For thermal radiation, the importance of the Mach disk relies in slowly moving fluid with high temperatures and pressures located behind the shock. This region become a very strong heat radiator. In the unshocked nozzle, the main source of gas radiation is located near the throat, where the highest temperatures and pressures are met, which explains the heat flux decrease with increasing x/L. However, the radiative heat flux originating near the throat hits the skirt walls with a small solid angle and travels through absorbing, emitting gases. On the other hand, the radiative heat flux originating from the Mach disk is located closer to the walls, with less participating gases to travel through: In the pocket behind the separation, the gas present is mainly nitrogen and thus transparent to radiation.

The first observation of the emission from the Mach disk is the influence on the flowfield. Indeed, the normal shock front looses energy and then is moved slightly downstream. Figure 7 shows a decrease in temperature and an increase in velocity induced by radiation at the position where the Mach disk was before activating the radiation model. Note that, to obtain this solution, the radiation term had to be updated every 200 iterations of the flow solver to avoid oscillations of the solution. In Fig. 7, value blanking is used to show only the relatively significant differences.

The second influence on the flowfield is a temperature increase just beside the film. The film itself is not heated by radiation because it does not contain water vapor, which is the only radiatively active specie in the calculation. However, a maximum increase of 30 K is observed, not very significant for the flow.

The second observation of the Mach disk emission is obvious in Fig. 8. The impinging radiative heat flux calculated for the shocked nozzle is compared to the unshocked nozzle heat flux, and the difference is plotted. The Mach disk emission not only increases the total radiative heat flux on the film-cooled section, but also makes it relatively constant around 240,000 W/m^2 because the heat flux radiated by the Mach disk increases with increasing abscissa. For $x/L > 0.75$, the main part of the radiative heat flux comes from the Mach disk region.

The wall temperature increase is plotted in Fig. 9. As mentioned, the cold gases have a much lower conductivity. Then according to the heat balance as stated in Eq. (3), this will imply a higher wall temperature for the same impinging radiative heat flux. For the shocked nozzle, the radiative heat is clearly increased, and a pocket of cold gas is filling the region downstream of the separation. This combination involves a wall temperature increase of 5–7 K before separation (hot film) and up to 140 K after the shock (cold air). Even if the heat balance stated is an approximation, because it should be

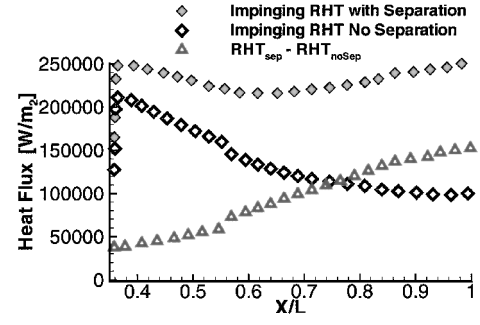

Fig. 8 Comparison of the impinging radiative heat flux with and without separation.

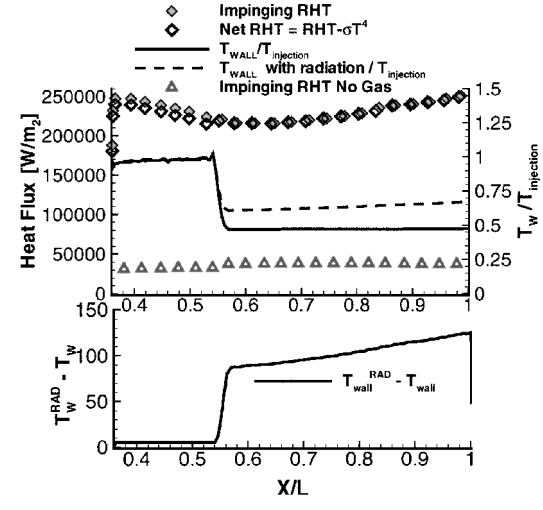

Fig. 9 Radiative heat flux and resulting wall temperatures for the sea level case.

coupled with the flow (the wall should be cooled by the slowly moving air), the effect of radiation can not be neglected. A wall temperature roughly 30% higher than the one calculated without radiation is observed.

In conclusion, in the case of shocked nozzle flow, neglecting radiative heat transfer leads to serious misapproximations, and even if the radiation calculation involves some uncertainty (nongray model, estimation of wall temperatures), the observations clearly show the

importance of radiation both for the flowfield and for the temperature evaluation.

Conclusions

The finite volume method for radiation with the spectral line-based weighted-sum of gray-gases has been implemented in a Navier–Stokes flow solver to calculate radiative heat transfer in rocket nozzles. A film-cooled nozzle was simulated at high altitudes, where the gases are not overexpanded, and at sea level, where the overexpansion of the gases create a shock system inside the nozzle. For the unshocked nozzle, the wall temperature increase by thermal radiation is negligible (~3 K). For the shocked nozzle, the radiative heat flux on the wall is much stronger because the Mach disk emission is as intensive as the combustion chamber gases emission. However, the film-cooled region before separation of the flow is weakly heated as in the high-altitude case. On the other hand, the shock fronts are pushed downstream due to their radiative energy loss, and the wall region behind the separation characterized by gases with low temperatures, low water vapor concentrations, and low velocities is warmed up. The wall temperature for this region is increased by up to 140 K. In conclusion, for large-scale nozzle calculations with film cooling, radiative heat transfer should not be neglected for the flow or for the estimation of the wall temperature.

Acknowledgments

This project was funded by Sweden's National Flight Research Program and was a cooperative project between Volvo Aero Corporation (VAC) and the Royal Institute of Technology, Stockholm, Sweden. H. Tamvel at VAC was the Technical Monitor. This work was supported with computing resources from the Swedish Council for Planning and Coordination of Research and Parallel Data Centrum at the Royal Institute of Technology. D. Eklund and L. Ljungkrona (VAC) are greatly acknowledged for their help, support, and comments during this work. The authors thank Arne Boman (VAC) who performed the computational fluid dynamics calculations.

References

[1]Ludwig, C. B., Malkmus, W., Reardon, J. E., and Thomson, J. A. L., *Handbook of Infrared Radiation from Combustion Gases*, NASA SP-3080, 1973.

[2]GreenWood, T. F., Lee, Y. C., Bender, R. L., and Carter, R. E., "Space Shuttle Base Heating," *Journal of Spacecraft and Rockets*, Vol. 21, No. 4, 1984, pp. 339–345.

[3]Sharma, S. P., and Whiting, E. E., "Modeling of Nonequilibrium Radiation Phenomena: An Assessment," *Journal of Thermophysics and Heat Transfer*, Vol. 10, No. 3, 1996, pp. 385–396.

[4]Nelson, H. F., "Radiative Heating in Scramjet Combustors," *Journal of Thermophysics and Heat Transfer*, Vol. 11, No. 1, 1997, pp. 59–64.

[5]Liu, J., and Tiwari, S. N., "Radiative Heat Transfer Effects in Chemically Reacting Nozzle Flows," *Journal of Thermophysics and Heat Transfer*, Vol. 10, No. 3, 1996, pp. 436–444.

[6]Raithby, G. D., and Chui, E. H., "A Finite Volume Method for Predicting Radiant Heat Transfer in Enclosures with Participating Media," *Journal of Heat Transfer*, Vol. 112, May 1990, pp. 415–423.

[7]Badinand, T., Eklund, D., and Fransson, T., "A Complete Procedure for Modelling Radiative Heat Transfer for Arbitrary Three-Dimensional Geometries for Gray Gases," 14th International Symposum on Air Breathing Engines Conf., IS-309, Sept. 1999.

[8]Eklund, D. R., Badinand, T., and Fransson, T., "A Numerical Study of Radiation Effects in Gas Turbine Combustion Chambers," AIAA Paper 98-3822, July 1998.

[9]Badinand, T., and Fransson, T., "Improvement of the Finite Volume Method for Coupled Flow and Radiation Calculations by the Use of Two Grids and Rotational Periodic Interface," *Proceedings of the Third International Symposium on Radiative Transfer* [CD-ROM], Begell House, New York, 2001.

[10]Denisson, M. K., and Webb, B. W., "The Spectral Line-Based Weighted Sum of Gray Gases Model for Arbitrary RTE Solvers," *Journal of Heat Transfer*, Vol. 115, Nov. 1993, pp. 1004–1012.

[11]Goutière, V., Liu, F., and Charette, A., "An Assessment of Real Gas Modelling in 2D Enclosures," *Journal of Quantitative Spectroscopy and Radiative Transfer*, Vol. 64, 2000, pp. 299–326.

[12]Badinand, T., and Fransson, T., "A Wavenumber Based Scaling Method for the Absorption Coefficient in the SLW Method for Strong Temperature and Pressure Gradient," *Proceedings of the Second Mediterranean Combustion Symposium*, edited by M. Kamel and M. S. Mansour, The Combustion Inst. and the International Centre for Heat and Mass Transfer, Ankara, Turkey, 2002, pp. 1170–1177.

[13]Badinand, T., and Fransson, T., "Influence of the Reference State in the SLW Model for Flows with Strong Temperature and Pressure Gradients," American Society of Mechanical Engineers, ASME Paper GT-2002-30230, June 2002.

[14]Rothman, L. S., Camy-Peyret, C., Flaud, J.-M., Gamache, R., Goldman, A., Goorvitch, D., Hawkins, R., Schroeder, J., Selby, J., and Wattson, R., "HITEMP, the High-Temperature Molecular Spectroscopic Database," *Journal of Quantitative Spectroscopy and Radiative Transfer* (to be published).

[15]Eriksson, L. E., "Development and Validation of Highly Modular Flow Solver Versions in G2DFLOW and G3DFLOW Series for Compressible Viscous Reacting Flow," Volvo Aero Corp., No. 9970-1162, Trollhättan, Sweden, 1995.

[16]Menter, F. R., "Zonal Two-Equation k–ω Turbulence Models for Aerodynamic Flows," AIAA Paper 93-2906, July 1993.

[17]Frey, M., and Hagemann, G., "Status of Flow Separation Prediction in Rocket Nozzles," AIAA Paper 98-3619, July 1998.

[18]Hadjadj, A., Nebbache, A., Vuillamy, D., and Vandromme, D., "Numerical Simulation of Flow Separation in Rocket Nozzle," *Mechanics Research Communications*, Vol. 24, No. 3, 1997, pp. 269–276.